# Characterization of a new external neutron beam facility at the Ohio State University

**Danyal Turkoglu · Joshua Burke · Radoslaw Lewandowski · Lei R. Cao**

**Abstract** A thermal neutron beam facility has been designed and implemented at the Ohio State University Research Reactor. A project is underway to construct a large vacuum chamber such that the facility could have neutron depth profiling and neutron radiography capabilities as intended. The neutron beam is extracted from the reactor through a neutron collimator emplaced in Beam Port #2. The neutron spectrum entering the neutron collimator was unfolded from foil activation analysis results and also simulated with a full reactor core model in the MCNP Monte Carlo code. The neutron collimator uses polycrystalline bismuth as a gamma ray filter and single-crystal sapphire as a fast neutron filter. The beam is defined by multiple 3.0 cm diameter apertures made of borated aluminum. Characterization of the beam was performed using foil activation to find the flux and a low-budget neutron imaging apparatus to see the beam profile. The modulation transfer function was calculated to offer insight into the resolution of the imaging system and the collimation of the beam. The neutron collimator delivers the filtered thermal neutron beam with a $\sim 4$ cm diameter and a thermal equivalent flux of $(1.27 \pm 0.03) \times 10^7$ n/(cm$^2$s) at 450 kW power at the end of the collimator.

**Keywords** Index terms: neutron collimator · Neutron imaging · Neutron depth profiling · MCNP · Neutron beam filters · Modulation transfer function

D. Turkoglu · J. Burke · R. Lewandowski · L. R. Cao (✉)
The Ohio State University, 201 W 19th Ave E402, Columbus, OH 43210, USA
e-mail: cao.152@osu.edu

## Introduction

Different from the power reactors, whose primary purpose is to produce heat to generate electricity, there are 240 [1] research reactors in the world with a primary function to provide a neutron source for research across multidisciplinary areas and a training and education platform for nuclear engineering professionals [2]. In addition to providing an intense neutron field for in-core materials irradiation, medical isotopes production and/or foil activation analysis (FAA), the external neutron beam is also bearing fruitful applications in materials, physics, archeology, biology, nuclear energy, and cross-disciplinary areas based upon the transduction of neutrons in terms of energy, angle, electric dipole, or quantum mechanical spin with the objects being investigated [3]. In most applications, the availability of a neutron beam that is thermal or sub-thermal, relatively free of gamma rays, and highly parallel is crucial in generating data with good signal-to-noise ratios. In the center of most infrastructures, an aluminum tube penetrates the reactor biological shielding wall with one end adjacent to the reactor core and the other end at an open space outside the reactor to provide a path in guiding neutrons for external usage. The main external instruments suitable for small-power University research reactors (URR) are neutron radiography/tomography [4], prompt gamma activation analysis (PGAA) [5], neutron depth profiling (NDP) [6, 7], intense positron source [8], and neutron diffraction tool. The North Carolina State University PULSTAR reactor recently added neutron radiography and tomography capabilities [9]. The Oregon State University TRIGA-II reactor recently added a single external neutron beam for PGAA and NDP capabilities [7]. The goal of this research is to build a neutron collimator and to characterize the resulting external neutron beam at

the Ohio State University Research Reactor (OSURR) with applications focused on energy-related studies, such as the lithium-, boron-, and/or sodium-containing advanced alloys and chemicals for nuclear energy and the Li-ion battery for electrical vehicles and hybrid electrical vehicles.

OSURR is a pool-type reactor licensed for continuous variable thermal power up to a maximum of 500 kW. The main applications of the reactor have been in-core or near-core irradiation for such purposes as NAA, evaluation of neutron and radiation-sensitive detectors, and radiation-damage evaluation. The core is comprised of fuel plates with open channels for natural circulation of light water. There is asymmetric reflection provided by graphite and light water (see Fig. 1). Beam Port #1 and Beam Port #2 are radial beam ports that terminate close to core with only a small gap filled by water. As both beam ports look directly at reactor fuel, fission neutrons and gamma rays are prevalent. A thermal neutron beam facility to expand upon the capabilities of the OSURR has been constructed using Beam Port #2, including the use of a large size, single-crystal sapphire as fast neutron filter and polycrystalline bismuth as a gamma filter. The characterization of the beam involves the modification of a position-sensitive neutron detector for imaging the beam profile, the use of the modulation transfer function (MTF) [10] for complementary quantification of the L/D ratio, and the
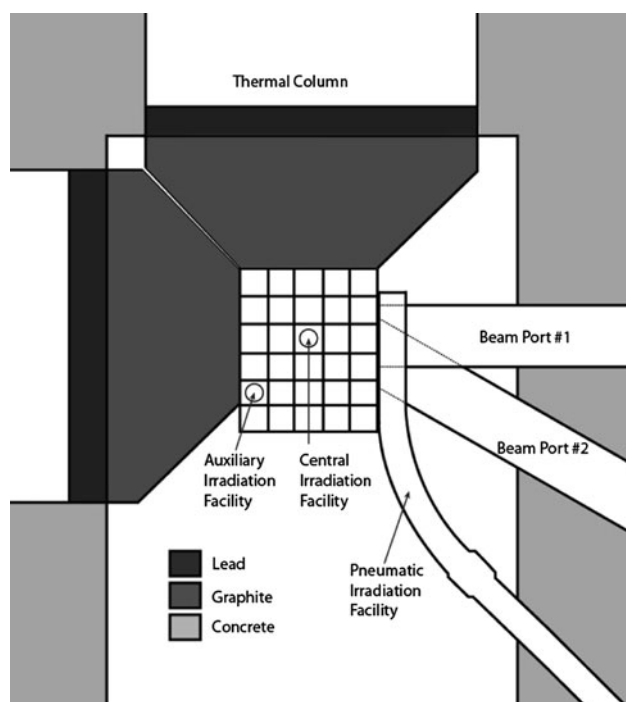


**Fig. 1** Schematic of the OSURR. The reactor core has asymmetric reflection, with graphite and light water used as moderators. Beam Port #2 is shown penetrating through the biological shielding and facing the core at a 30° angle

measurement of neutron energy spectrum and its comparison with Monte carlo (MC) simulation.

## Neutron collimator design

Central to this facility is a neutron collimator designed to filter and shape a small-sized external neutron beam. The neutron collimator is an aluminum tube housing the components and is emplaced into Beam Port #2, which faces the reactor core at a 30° angle. The first component closest to the core is a single block of polycrystalline bismuth, 12.82 cm in diameter and 10.0 cm in length, employed to reduce the gamma ray content significantly. The multi-piece, single-crystal sapphire with a total length of 12.7 cm and 10.16 cm in diameter follows with the function of reducing fast neutron content while allowing a high transmittance of neutrons in the wavelength range of interest (0.12–0.25 nm). The filtration of fast neutrons is a result of the neutron wavelength dependency of cross-sections for the sapphire which are at a minimum of about 1 barn at thermal energies and significantly higher at about 10 barns for neutron energies greater than 1 eV [9]. The cross-sections are reduced for neutron energies less than 0.1 eV as much of the coherent Bragg scattering is disallowed when the crystal is preferentially oriented [11]. Stamatelatos and Messoloras [12] found the optimum thickness of the sapphire filter to be 15.0 cm. They showed that sapphire of this thickness gives 62% transmission of neutrons with 0.11 nm wavelength and 76% transmission for 0.25 nm neutrons while only 3% of fast neutrons are transmitted. Due to its high efficiency at room temperature, the sapphire is commonly selected as a filter for thermal neutrons compared with cryogenically cooled silicon and quartz single-crystals. The implementation of filters to reduce energetic neutrons is not only beneficial in improving radiographic characteristics or reducing noise in other measuring techniques, but also in decreasing the amount of fast neutron shielding required for adhering to requirements imposed by neighboring devices or by regulations for doses to personnel.

The collimation of neutrons (and remaining gamma rays for that matter) is achieved by a series of parallel apertures consisting of borated aluminum and lead. The final aperture is epoxy containing lithium enriched in $^6$Li, which has a relatively high thermal neutron cross-section of 940 barns and more importantly, does not produce secondary capture gamma rays as $^{10}$B does (478 keV). Glass mixed with fused silica, alumina and $^6$Li-carbonate is being fabricated and will replace the last aperture, aiming to eliminate the 2.2 MeV prompt gamma rays from activated hydrogen in epoxy. The apertures are 30 mm in diameter. The principle is that only neutrons traveling parallel to the collimator and

down the centerline can be delivered to the sample. Figure 2 shows the collimator tube alongside its internal components. It is designed to be evacuated to eliminate the attenuation of the beam by air.

A functioning beam facility requires the ability to toggle the beam on and off and for the beam to be shielded in both of these states. A beam shutter was designed to shield the neutron beam adequately when the facility is not in use or when sample changes are being performed. The beam shutter is comprised of three main features: (1) a high-boron content borated aluminum disk to absorb essentially all thermal neutrons; (2) layers of five weight percent borated polyethylene for fast neutron shielding; and (3) a shell of lead with 15.24 cm on the backside for gamma shielding. The borated aluminum disk is recessed 10.16 cm into the borated polyethylene so that the backscatter of neutrons is reduced. A lift column raises the beam shutter vertically, such that the beam can pass through the gap below the beam shutter. Figure 3 illustrates the operation of the beam shutter with the facility setup for a neutron imaging experiment. The beam stop is of the same design as the beam shutter except that $^6Li$ in epoxy replaced the borated aluminum in an effort to reduce radiation background by eliminating the 478 keV gamma rays from $^{10}B$.

The neutron spectrum and flux near the core in BP #2 were determined with NAA of bare and cadmium-covered wires and SAND-II to unfold the spectrum. SAND-II is a computer code which uses an iterative method to find the best fit of spectra based upon the activation of foils and the cross-section libraries of the given materials [13]. Gold, cobalt, and copper were selected to act as thermal and intermediate energy neutron detectors according to ASTM E 261 [14]. The MCNP5 MC [15] code was used to simulate the shape of the spectrum at the same location near the core as in the experiment. The shapes of spectra were similar as shown in Fig. 4, but the NAA measurement underrepresented the contribution of the fast flux. Since BP #2 looks directly at the reactor fuel, the fission neutron content is prevalent. The inclusion of a fast neutron detector specimen, such as $^{58}Ni$ in the experiment, could have more accurately fit the spectra. The experiment found the total flux to be $\sim 5 \times 10^{12}$ n/(cm$^2$s) at 450 kW power,



**Fig. 3** The beam facility set up for an imaging experiment to test and characterize the neutron beam. The lift column has the beam shutter raised such that the beam passes through the gap (1). The beam interacts with the light-tight imaging box (2), and the beam stop (3) terminates it

with about 62% considered to be slow neutron content (defined here with energies less than 0.4 eV). By contrast, the MCNP simulation found only 41% to be slow neutron content. The thermal equivalent flux, which accounts for the spectrum of neutrons by equating the reaction rate caused by the total flux to the thermal flux needed to produce it, was found to be $2.5 \times 10^{12}$ n/(cm$^2$s) at full power. By definition, the cadmium ratio is the ratio of the reaction rate in a bare gold foil to that of a cadmium-covered foil. It is an important metric related to the proportion of neutrons that are considered slow since the cadmium has a sharp cut-off in cross-sections for energies above 0.4 eV. This was found to be 6.5 by taking the ratio of the specific activity of bare gold wire to that of the cadmium-covered gold wire.

## Neutron imaging experiment

For testing and characterizing the neutron beam, the collimator was emplaced in Beam Port #2 and the beam shutter and beam stop were set up as shown in Fig. 3. A real-time neutron imaging apparatus previously designed at the National Institute of Standards and Technology for

**Fig. 2** The collimator components, separated by aluminum spacers, alongside the aluminum tube that encases them. The internal components are: (1) Poly-crystal bismuth, (2) Single-crystal sapphire in a borated polyethylene holder, (3) Borated aluminum aperture, (4) Lead aperture, and (5) Lithiated epoxy aperture
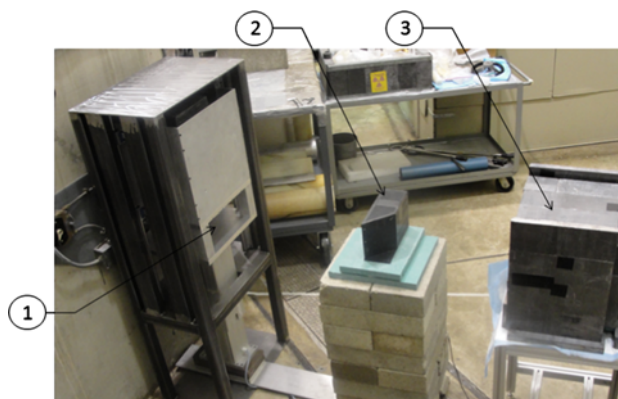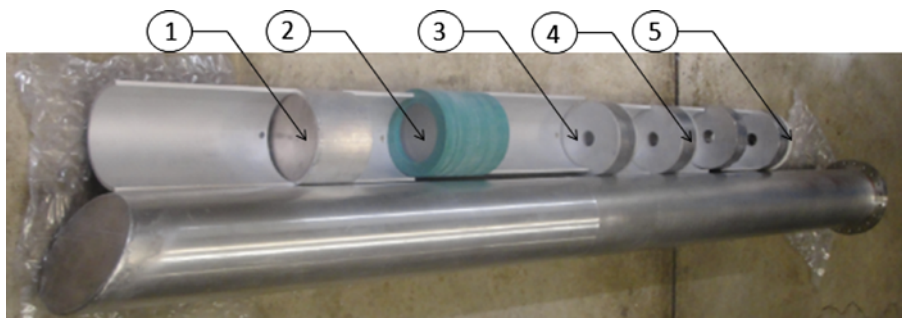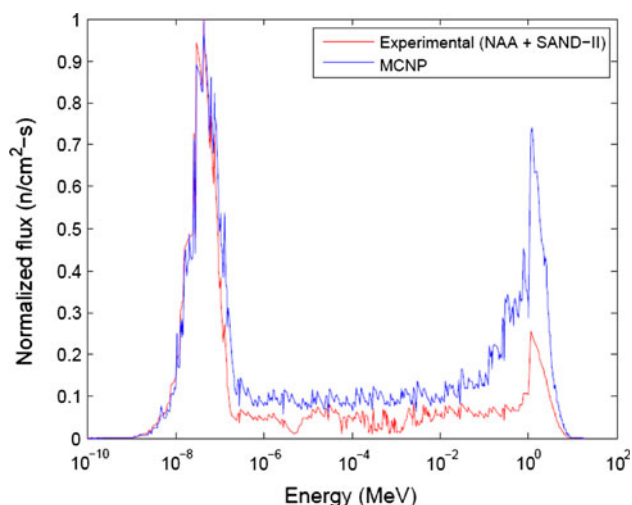
**Fig. 4** Comparison of the neutron spectrum determined experimentally to that simulated by MCNP near the reactor core

finding the focal spot of a neutron lens [8] was modified for the purposes of finding the beam profile and gaining insight into the divergence of the beam by measuring the resolution of the system. The main components of the imaging device are a light-tight aluminum box, the scintillation screen, a front surface mirror made of $^6$Li-containing glass, and the charged-coupled device (CCD) digital camera, as shown in Fig. 5. The scintillation screen is a ZnS phosphor with a thin coating of $^6$Li that converts neutrons into charged particles. The excitation of the phosphors by the alpha and triton particles from $^6$Li results in the emission of visible green light, which is reflected off the mirror at a 45° angle into the CCD camera. The $^6$Li-containing mirror not only allows the camera to be out of the high radiation beam, but also absorbs thermal neutrons with the consequence of reducing activated gamma rays and minimizing the number of scattering neutrons, which would adversely affect the silicon-based CCD camera. Neutron imaging at a
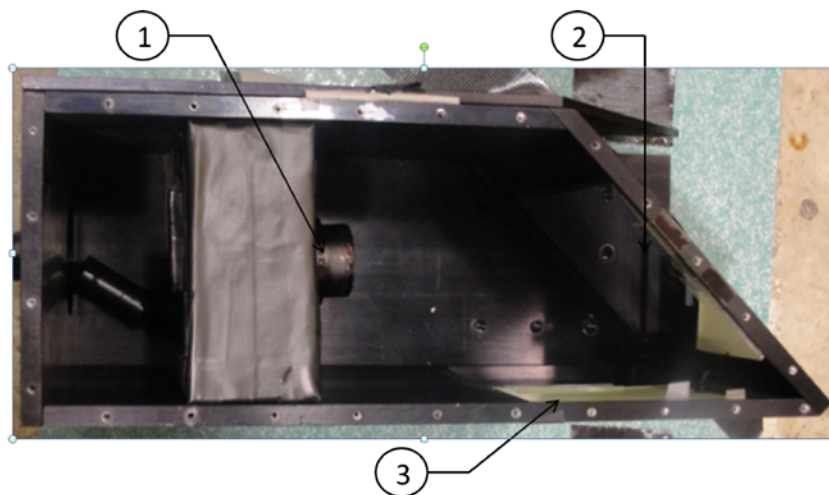
URR that normally has relatively lower neutron flux requires the use of image intensifiers or extremely long-exposure times on the order of minutes to hours to allow enough light collection to discern differences without the interference of background. Consequently, a commercial low-cost Canon® digital camera was chosen because of the availability of the open-source code that could modify the exposure time of the camera. The neutron imaging techniques applied for this experiment are low-budget but capable of generating moderate high-quality, digital neutron radiography pictures.

A crosshair made of cadmium, an element opaque to thermal neutrons, was placed over the center of the aluminum thin window of the collimator as shown in Fig. 6. As this corresponds to the center of the beam, locating the beam was made easy by the shadow that the crosshair cast on the imaging box. Figure 6 also shows a picture of the beam with the camera exposure set to 256 s. The umbra is the focused and most intense part of the beam. The thermal neutron equivalent flux at this part of the beam was measured with NAA of a gold foil placed over the aluminum thin window and found to be $(1.27 \pm 0.03) \times 10^7$ n/(cm$^2$s) at 450 kW power. Typically radiography pictures are converted to gray scale to acquire an intensity image in which individual pixel values range from a minimum of 0 to a maximum of 255 or a camera collecting only one color of light is used. For this case with the scintillation screen emitting green light, the green component of the digital images was used to create the beam image as it preserved the same size and shape as the gray scale image but with less noise. The beam intensity profile is shown in Fig. 7. The beam profile at the end of the collimator but before the aluminum thin window was simulated and also shown in Fig. 7. The circular neutron beam projected on the image plane was found to be $\sim 4$ cm. The divergence of the beam was calculated to be 2.39°.

**Fig. 5** The light-tight imaging box opened up to show the Canon CCD camera (*1*), the mirror (*2*), and the ZnS phosphor scintillation screen (*3*)
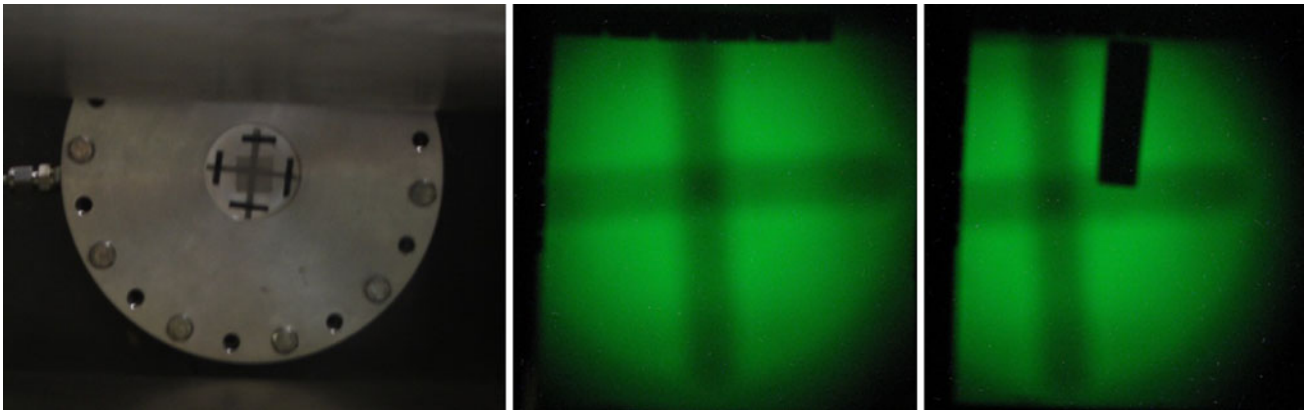
**Fig. 6** The cadmium crosshair put over the aluminum thin window cast a shadow on the imaging box (*left*). The image of the beam taken with a 256 s exposure time (*middle*). The picture had a sharp edged piece of cadmium placed on the outside of the imaging box so that the resolution of the imaging system could be calculated using the MTF approach (*right*)
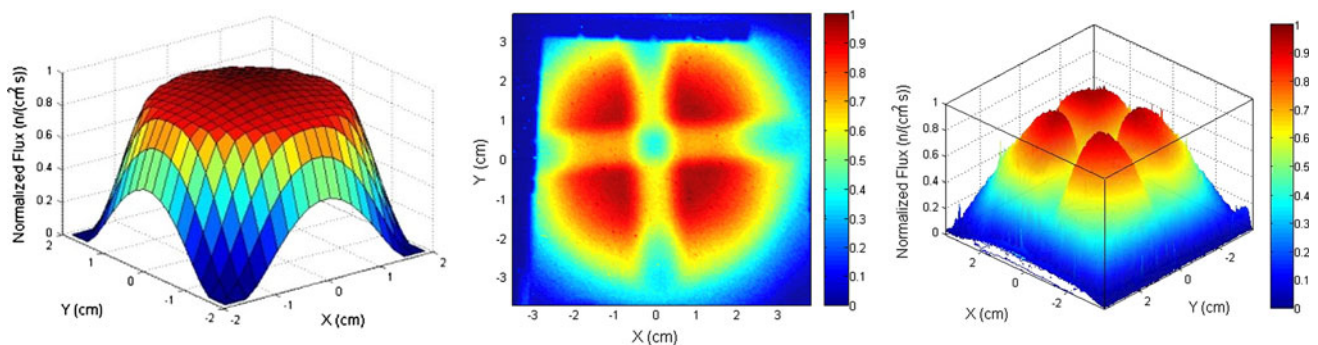


**Fig. 7** The beam intensity profile before the aluminum thin window simulated in MCNP (*left*). The beam size is indicated in the 2-D intensity image (*middle*) and in 3-D (*right*) for the imaging experiment with the cadmium cross-hair

## Modulation transfer function

A small edge-polished cadmium strip was placed against the aluminum window of the imaging box, giving rise to a projected shadow-image of the cadmium on the scintillation screen. The overall system resolution was evaluated quantitatively from the blurred edge with which the Modulation transfer function (MTF) was calculated. The MTF measures the extent of the amplitude attenuation when signals with varying frequencies pass through a linear system. It has been widely applied in evaluating X-ray medical imaging system and has also gained acceptance in characterization of the neutron imaging facility [16]. The overall MTF can be represented as a cascade of its individual components; in our system, this includes the neutron collimator, the scintillation screen, and the digital camera. The MTF of the scintillation screen and the digital camera are superior to the MTF represented by the neutron beam, indicating the unsharpness caused by the neutron beam is the dominating factor in determining the system resolution.

Therefore, a proper measurement of MTF using a neutron opaque object with a sharp edge will provide a fair estimation of how parallel a neutron beam is a property L/D ratio normally describes.

The calculation of the MTF is implemented in the following steps: (1) Extract a relatively uniform edge block; (2) Apply a median filter; (3) Produce an array of edge profile by averaging 100 rows crossing the edge; (4) Differentiate the edge profile to form a line profile; (5) Apply fast fourier transform (FFT) to the line profile to obtain the MTF. Figure 8 shows the calculated MTF of our system. The frequency step represented by each pixel is obtained by knowing the fact that an array of 165 pixels covers the 8.8 mm cadmium strip, which gives an effective pixel size of 0.053 mm. The sampling frequency, therefore, is 18.9 line pair/mm (lp/mm) corresponding to a cut-off, or Nyquist frequency of 9.5 lp/mm. The 10% MTF in Fig. 8 corresponds to 0.6 lp/mm (or 1.67 mm), which indicates the resolution of the system and serves as the approximation on the figure-of-merit of the neutron collimation.
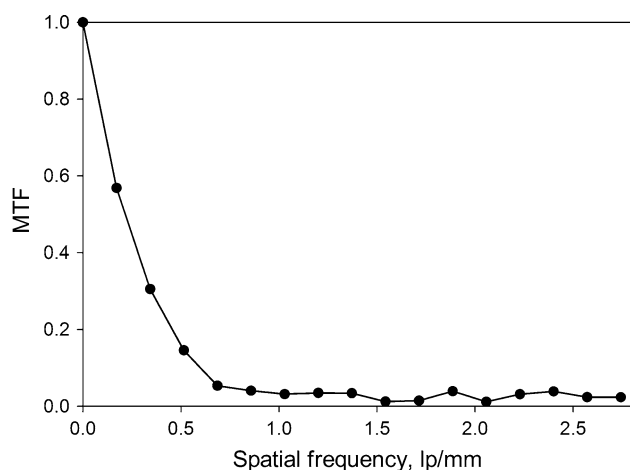
**Fig. 8** The MTF of the imaging system and the approximation of the MTF contributed by the neutron collimator

## Applications

At present, a project is underway to add a large vacuum chamber suited for neutron depth profiling (NDP) and neutron imaging as primary applications to the facility. The NDP is a unique and non-destructive analytical method that relies on charge-particle emitting exoergic nuclear reactions. Such neutron-induced nuclear reactions are particularly prone to occur for a few isotopes among light-weighted elements, such as boron and lithium, which, generally speaking, are difficult to measure by other methods, such as X-ray fluorescence (XRF), Rutherford back-scattering (RBS), and Nuclear reaction analysis (NRA). Even with a small university reactor, the NDP technique can be effectively applied as the isotopes of interest have large cross-sections that can be seen with the flux level. However, to enhance detection efficiency significantly and thereby reduce the counting time, the NDP facility will be equipped with a total of eight charged particle detectors at the same solid angle to the sample and an all-digital spectroscopy to aid in the consolidation of the data streams.

NDP could possibly determine sodium penetration and diffusion within the near-surface region of the cladding materials that contact liquid sodium. This capability could help to uncover the fundamental material properties behind liquid metal embrittlement (LME). Naturally occurring sodium is 100% $^{23}$Na, an isotope that exhibits a very small thermal neutron capture cross-section ($\sim 0.53$ barns) with gamma ray emission. However, the artificial isotope $^{22}$Na undergoes the reaction $^{22}$Na (n,p) $^{22}$Ne with a neutron cross-section of 28,897 barns, making it highly sensitive to concentration versus depth determination by NDP. The $^{22}$Na is a moderately long-lived $\beta^+$ emitter with a half-life of 2.6 years, which makes it preferable as a labeling atom to mimic sodium interaction with reactor materials.

## Conclusion

An external neutron beam is designed, constructed, and characterized with advanced neutron imaging techniques for viewing the beam profile and quantification of beam divergence by adoption of MTF instead of the traditionally used L/D ratio. The major part of the facility is a new collimator consisting of single block poly-crystal bismuth as a gamma filter, a multi-piece single-crystal sapphire as a fast neutron filter and multiple borated neutron aperture in defining a thermal neutron beam of 30 mm in diameter. The thermal flux is found to be $(1.27 \pm 0.03) \times 10^7$ n/(cm$^2$s) with gold foil activation at the exit window of neutron collimator. The neutron energy spectrum was measured with foil activation and spectrum deconvolution and the results were compared against the MCNP-based whole core simulation. The primary focus of this research facility is the application of neutron-based analytical technologies to the characterization of advanced energy-related materials, including materials used in the advanced nuclear reactors and the Li-ion battery.

## References

1. Nuclear Research Reactors (2009) IAEA, Austria. http://nucleus.iaea.org/RRDB/RR/ReactorSearch.aspx. Accessed 15 May 2011
2. Adelfang P, Ritchie I (2003) Overview of the status of research reactors worldwide. In: The 25th international meeting on reduced enrichment for research and test reactors (RERTR), Chicago, Illinois, pp 12–23
3. Prask HJ, Rowe JM, Rush JJ, Schroder IG (1993) The NIST cold neutron research facility. J Res Natl Inst Stand Technol 98:1–15
4. Cao L (2007) Development of a high spatial resolution neutron imaging system and performance evaluation. The University of Texas, Austin
5. Révay Z, Harrison RK, Alvarez E, Biegalski SR, Landsbergern (2007) Construction and characterization of the redesigned PGAA facility at The University of Texas at Austin. Nucl Instrum Methods Phys Res A 577(3):611–618
6. Whitney SM (2008) Neutron depth profiling benchmarking and analysis of applications to lithium ion cell electrode and interfacial studies research. The University of Texas, Austin
7. Robinson JA, Hartman MR, Reese SR (2010) Design, construction and characterization of a prompt gamma activation analysis facility at the Oregon State University TRIGA reactor. J Radioanal Nucl Chem 283(2):359–369
8. Moxom J, Hathaway AG, Hawari AI (2007) Out of core testing of the North Carolina State University PULSTAR reactor positron beam. IEEE Nucl Sci Symp Conf Rec 1–11:2343–2348
9. Mishra KK, Hawari AI, Gillette VH (2006) Design and performance of a thermal neutron imaging facility at the North Carolina State University PULSTAR reactor. Nucl Sci IEEE Trans 53(6):3904–3911
10. Gagne RM, Boswell JS, Myers KJ (2003) Signal detectability in digital radiography: spatial domain figures of merit. Med Phys 30(8):2180–2193
11. Nieman HF, Tennant DC, Dolling G (1980) Single-crystal filters for neutron spectrometry. Rev Sci Instrum 51(10):1299–1303

12. Stamatelatos IE, Messoloras S (2000) Sapphire thickness optimization in neutron scattering instruments. Rev Sci Instrum 71(1):70–73

13. Griffin PJ, Kelly JG, VanDenburg JW (1994) User's manual for SNL-SAND-II code. Sandia National Laboratory, Albuquerque

14. ASTM Standard E 261–03 (2003) Standard practice for determining neutron fluence, fluence rate, and spectra by radioactivation techniques. ASTM International, West Conshohocken

15. X-5 Monte Carlo Team (2005) MCNP—a general Monte Carlo N-particle transport code, Version 5. Los Alamos National Laboratory, Los Alamos

16. Anderson IS, McGreevy RL, Bilheux HZ (2009) Neutron imaging and applications. Springer, New York